

1 **Sediment Yield and its Interannual Variability are**
2 **Underestimated in Supply-Limited Mountain Basins**
3 **with Short Records**

4 **Jacob Hirschberg^{1,2}, Brian W. McArdell¹, Georgina L. Bennett³, and Peter**
5 **Molnar²**

6 ¹WSL, Swiss Federal Institute for Forest, Snow and Landscape Research, Birmensdorf, Switzerland

7 ²Institute of Environmental Engineering, ETH Zurich, Zurich, Switzerland

8 ³Geography, University of Exeter, Exeter, United Kingdom

9 **Key Points:**

- 10 • Long-term sediment flux simulations (10k years) at hourly resolution are studied
11 under stochastic forcing
- 12 • Sediment yield estimates from short records are highly uncertain and likely un-
13 derestimated
- 14 • The actual timing of sediment input events is not preserved in the sediment yield

Corresponding author: Jacob Hirschberg, jacob.hirschberg@wsl.ch

Abstract

Climate and sediment supply are critical factors for the sediment output of geomorphic systems. It is known that non-linearities between forcing and sediment mobilization may lead to dampened or shredded environmental signals in sediment flux measurements. But it is unclear under which circumstances environmental signals, such as extreme events or climate change, are transmitted and measurable downstream. We used a sediment cascade model and a stochastic weather generator to quantify climate forcing effects under a range of sediment supply regimes in a debris-flow catchment in the Swiss Alps (Illgraben). Sediment yields estimated from short records have high uncertainties both in terms of mean and interannual variability, and tend to be underestimated especially in supply-limited systems, where also long-term memory effects driven by sediment storage are evident. Consequently, climate change impact assessments based on short duration records may be grossly inaccurate, and should be extended with uncertainty estimation.

Plain Language Summary

Whether or not climate change is measurable in the sediment output of a basin is a timely question. Climate has an important role for processes related to sediment production and transport. However, because relations between these are complex and often non-linear, it is questionable if environmental signals such as climate change are also transmitted and measurable in the downstream sediment transport. We used a sediment cascade model and a stochastic weather generator to study the detectability under a range of conditions such as different sediment sampling durations and different mean erosion rates in a debris-flow catchment in the Swiss Alps (Illgraben). We show that sediment yields estimated from short duration records are highly uncertain and that transient sediment supply introduces long-term memory effects. Consequently, climate change impact assessments based on short duration records may be grossly inaccurate, and should be extended with uncertainty estimation.

1 Introduction

The study of erosion rates is fundamental for understanding landscape response to environmental signals such as climate change (e.g., Molnar & England, 1990; Bookhagen & Strecker, 2012; Adams et al., 2020), land use change (e.g., Borrelli et al., 2017), deciphering sedimentary records (e.g., Castelltort & Van Den Driessche, 2003), and for predicting hazards and risk connected to sediment transport processes (Jakob et al., 2005) or riverine ecological habitat (Evans et al., 2006). Spatially averaged erosion rates are usually defined for a given area and at different timescales. Short-term erosion rates can be inferred from measured sediment loads with a representative timescale of years to decades (e.g., Fuller et al., 2003). Long-term estimates, averaged over $\sim 10^5$ -years, are commonly inferred from sediment tracing, e.g., by cosmogenic radionuclide concentrations such as ^{10}Be in alluvial sediments (Brown et al., 1995). Comparing such short- and long-term sediment yield estimates has revealed some discrepancies depending on basin size and the dominant erosional process (see Covault et al., 2013, and references therein). Short records are often missing erosional pulses resulting from rare events such as large landslides or extreme rainfall (Kirchner et al., 2001; Schaller et al., 2001; Tomkins et al., 2007). This leads to the underestimation in sediment yields especially in small, natural basins with little opportunity for sediment storage, while larger basins buffer these pulses in floodplains (Wittmann et al., 2011). The variable timescales of sediment production and transfer therefore present significant challenges for observation and prediction.

Observational and modelling challenges in geomorphic systems also arise from non-linearities due to the complex relationships between climatic forcing, hydrological and

64 sediment connectivity, the biosphere and the different geomorphic thresholds involved
65 in sediment production, storage and transport (e.g., Phillips, 2003; Lancaster & Case-
66 beer, 2007; Van De Wiel & Coulthard, 2010; Coulthard & Van De Wiel, 2013; Pelletier
67 et al., 2015). Recent work highlights the importance of the frequency and magnitude of
68 forcing variables compared to system response timescales (Jerolmack & Paola, 2010) and
69 the signal preservation in the stratigraphic records by undisturbed deposition in short
70 intervals between erosion events (Sadler & Jerolmack, 2015; Paola et al., 2018; Ganti et
71 al., 2020). These perspectives are drawn from observations, theoretical constructs and
72 simple models, e.g., the sandpile model (Bak et al., 1987), and they illustrate the poten-
73 tial impact of the timing of sediment supply and export on basin sediment yields. More
74 complex numerical models are increasingly used to study the non-linear response of sed-
75 iment flux to variability in forcings (e.g., Tucker & Bras, 2000; Van De Wiel & Coulthard,
76 2010; Coulthard & Van De Wiel, 2013; Godard & Tucker, 2021). The effect of mass move-
77 ments and their impact on sediment fluxes on shorter timescales has received less atten-
78 tion. Yet modelling tools are most appropriate to capture the cause-and-effect relations
79 in geomorphic systems, necessary for climate change impact and hazard assessments, and
80 for designing sampling strategies and hazard mitigation structures.

81 Herein we focus on steep headwater catchments, which are often characterized by
82 mass-wasting processes such as landslides and debris flows (e.g. Dietrich & Dunne, 1978;
83 Bennett et al., 2013), fed to the channel in a stochastic manner (Benda & Dunne, 1997a,
84 1997b), and affecting the downstream sediment flux (Hovius et al., 1997). We use a stochas-
85 tic process-informed geomorphic modelling perspective to show how (a) sediment sup-
86 ply limitations cause bias and uncertainty in sediment yield estimates; (b) short records
87 affect debris-flow magnitude-frequency distributions; (c) memory effects in sediment yields
88 contrasts in supply-limited and transport-limited systems; and (d) the exact timing and
89 magnitudes of sediment inputs are shredded in the sediment yield.

90 2 Experimental setup

91 2.1 Geomorphic System and Climate Forcing Models

92 We coupled the SedCas sediment cascade model (Bennett et al., 2014) and the AWE-
93 GEN stochastic weather generator (Fatichi et al., 2011) to simulate hydrological and sed-
94 iment fluxes at the highly active Illgraben debris-flow torrent (4.8 km²), located in the
95 Swiss Rhône Valley and producing ~ 5 debris flows yearly on average (Hirschberg, Badoux,
96 et al., 2021). This model setup was calibrated by (Hirschberg, Fatichi, et al., 2021) against
97 observed climate and debris-flow magnitudes to assess climate change impacts on sed-
98 iment yield and debris-flow activity in the 21st century and also provided a detailed de-
99 scription of the calibration, validation and sensitivity analysis of the entire model chain
100 (see the article supplement). Here, we ran simulations at high temporal resolution (hourly)
101 while spanning geomorphologically relevant timescales (10k years) and a range of climatic
102 and sediment supply conditions.

103 SedCas is a conceptual geomorphic system model where the sediment production
104 rates by hillslope landslides (triggered by frost-weathering, rainfall, or randomly) are stochas-
105 tic and drawn from a prescribed probability distribution (Bennett et al., 2012). These
106 landslides provide sediment to the channel and can be re-mobilized and transported out
107 of the catchment by debris flows and fluvial processes, which are simulated with a con-
108 ceptual hydrological model.

109 AWE-GEN is used for the stochastic climatic forcing of SedCas. It produces hourly
110 time series of correlated weather variables (e.g., precipitation, air temperature) at the
111 point scale (Fatichi et al., 2011). It was calibrated against 30 years of observations from
112 a weather station in the vicinity (11 km) of the catchment.

113 Coupling these models reflects the observation that climate and landslides (sedi-
 114 ment input) are stochastic forcings in geomorphic systems (Benda & Dunne, 1997a, 1997b)
 115 and that the resulting debris-flow activity (sediment output) depends not only on the
 116 recurrence interval of climatic thresholds triggering debris flows, but also on the sedi-
 117 ment recharge to the channel (Bovis & Jakob, 1999; Jakob et al., 2005). In the 10k-year
 118 simulations, the model parameters remain unchanged and the forcings from climate and
 119 sediment recharge are therefore stationary. Hence, the estimated mean sediment yields
 120 from the full simulations represent the equilibrium state. The estimated uncertainties
 121 result from temporal variability in climate and sediment input, and geomorphic thresh-
 122 olds.

123 2.2 Modelled Scenarios

124 We ran SedCas with six scenario setups, as summarized in Table S1. The calibrated
 125 setup with frost-weathering as the main hillslope sediment supply mechanism (Bennett
 126 et al., 2013) and 25 yearly sediment recharge events on average served as a reference (re-
 127 ferred to `thermal_ls25` hereafter). To study the effect of the timing (seasonality) of sedi-
 128 ment recharge, and decouple it from air temperature, we ran simulations with the same
 129 number of hillslope landslides triggered by rainfall and randomly (`rainfall_ls25` and `ran-
 130 dom_ls25`). For simulating sediment supply-limited conditions we assumed that the prob-
 131 ability distribution of landslide magnitudes remains fixed, but we reduced the number
 132 of yearly generated landslides from 25 to 16 and 8 with the frost-weathering mechanism
 133 (`thermal_ls26` and `thermal_ls8`). This resulted in decreased erosion rates by 1/3 and 2/3,
 134 respectively. We additionally considered a transport-limited scenario to quantify signals
 135 in the sediment yield introduced by interannual climate variability alone.

136 All scenario runs were forced with the same 10k-year hourly climate simulated with
 137 AWE-GEN and therefore the hydrological variables (e.g., snowcover, soil moisture, dis-
 138 charge, etc.) are identical among the scenarios. When the condition for a hillslope land-
 139 slide was met, the magnitude was sampled from the same distribution in every scenario
 140 (Figure 1a). However, depending on the scenario the number of landslides can differ. To
 141 enforce 25, 16 and 8 landslides on average per year, the temperature threshold for the
 142 onset of frost-weathering was adjusted (Table S1). The simulated channel sediment stor-
 143 age develops in cycles of transport-limited and supply-limited conditions (Figure 1b) and
 144 confirms that the long-term sediment delivery ratio goes to 1 (i.e. no long-term storage).
 145 The differences in sediment supply result in distinct distributions of annual sediment yields.
 146 The more supply-limited, the more right-skewed is the sediment yield distribution and
 147 the lower the mean (Figure 1c).

148 2.3 Analysis of Long-Term Simulations

149 Each scenario simulation (Table S1) was resampled with different sampling dura-
 150 tions to quantify uncertainties in annual sediment yields and their interannual variabil-
 151 ity. The full time series was split into periods from 1 to 100 years, and the mean and vari-
 152 ance of the sediment yield were estimated for each subset. The uncertainties in these es-
 153 timates were computed to analyze (a) the effects of short records on the sediment out-
 154 put and (b) the detectability of differences in sediment input between the scenarios.

155 Sediment storage is a source of non-linearity in geomorphic systems (Phillips, 2003).
 156 To identify and quantify the long-term memory effects in sediment yields induced by tem-
 157 porary sediment storage, we analyzed long-term correlation in sediment yields using de-
 158 trended fluctuation analysis (DFA, Peng et al., 1994) using Python (Rydin & Hassan,
 159 2021). DFA is a technique to identify scaling properties in fluctuating or non-stationary
 160 time series, e.g., precipitation (Matsoukas et al., 2000) or temperature (e.g., Koscielny-
 161 Bunde et al., 1998; Shao & Ditlevsen, 2016). The mean of the detrended variance scales
 162 with sampling record duration s as $\overline{F(s)} \propto s^\alpha$. Applying DFA on uncorrelated random

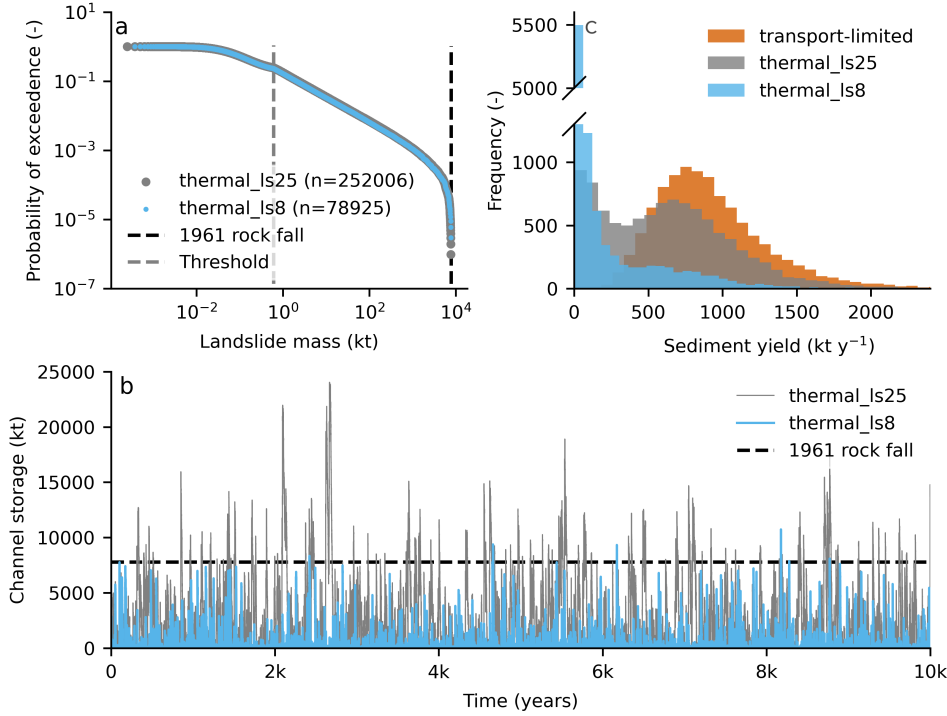


Figure 1. Comparison of different sediment supply scenarios (see Table S1); “thermal_ls25” is the original model setup and calibrated for Illgraben; “transport-limited” and “thermal_ls8” are hypothetical scenarios with unlimited and reduced sediment supply, respectively. (a) Magnitude-frequency distributions of the hillslope landslides generated with SedCas (Bennett et al., 2012). (b) Example time series of the channel sediment storage available for mobilization, with indication of the largest observed rockfall in 1961. (c) Histograms of simulated annual sediment yields.

series (white noise) results in $\alpha = 0.5$ (Kantelhardt et al., 2002). Time series with long-term memory manifest in $\alpha > 0.5$ (Figure S2a). When plotting α as a function of s , i.e. the local slope from the $s-\overline{F}(s)$ plots, the representative timescales and scaling properties can be identified visually (Figure S1 Bryce & Sprague, 2012). We also examined the presence of long-term memory by fitting an ARFIMA model to the sediment yield time series and estimated the differencing order d which is related to the Hurst exponent H as $d = H - 0.5$, where $d > 0$ ($H > 0.5$) is also indicative of long-term memory (Montanari et al., 1997).

3 Results

3.1 Effects of Short Records on Sediment Yield Estimates

Analyses are presented for annual sediment yields and corresponds to the mean mass of sediment exported from the catchment by debris flows per year (unless declared differently). The estimated mean annual sediment yield $\hat{\mu}$ can be both greatly over- or underestimated in all scenarios if based on short records (Figure 2a). The uncertainty is largest for thermal_ls25, where $\hat{\mu}$ can be biased by a factor of ~ 2 even after 30 years of measurements. Although uncertainty bounds of $\hat{\mu}$ for different scenarios may overlap even

179 after 50 years, there are distinct equilibria. Thus, sediment-supply regime changes are
 180 likely to be identified after 30 years of sampling in this system. Underestimating $\hat{\mu}$ based
 181 on short records is most likely for the strongly supply limited thermal_ls8.

182 The rate at which the uncertainty in $\hat{\mu}$ drops is related to the effect of record du-
 183 ration, interannual variance, and interannual memory on the standard error of $\hat{\mu}$ (Montgomery
 184 & Runger, 2018). Similarly to $\hat{\mu}$, the estimate of the interannual variance (standard de-
 185 viation) of annual sediment yields $\hat{\sigma}$ is affected by record duration, but with more over-
 186 lap between the scenarios (Figure 2b). However, $\hat{\sigma}$ is underestimated in all scenarios for
 187 short records, and this effect is stronger for supply-limited scenarios. As a consequence,
 188 in order to not underestimate $\hat{\sigma}$, observations of ~ 30 years are necessary especially for
 189 supply-limited conditions. Repeating the same analysis for the annual total sediment yield
 190 (including fluvial transport) and the annual number of debris flows resulted in the same
 191 patterns (Figures S2, S4).

192 The scenarios with the same number of landslides as thermal_ls25 but different trig-
 193 gering mechanisms showed very similar results (Figures 2c, S2). These scenarios differ
 194 in the seasonality of sediment recharge, but such high-frequency variations were not dis-
 195 tinctly transmitted to the outlet, and therefore invisible in the annual sediment yields.
 196 Comparing the thermal scenarios ls_8, ls_16 and ls_25 shows a clear effect of reduced sed-
 197 iment supply in diminishing mean sediment yields and increasing interannual variabil-
 198 ity. Although the climate forcing remained the same among the scenarios, by altering
 199 sediment supply, the coefficient of variation (CV) increased from 0.7 in the transport-
 200 limited case, to ~ 1 for the ls25 scenarios and to 1.5 and 2.3 for the more supply-limited
 201 scenarios (Figure 2c).

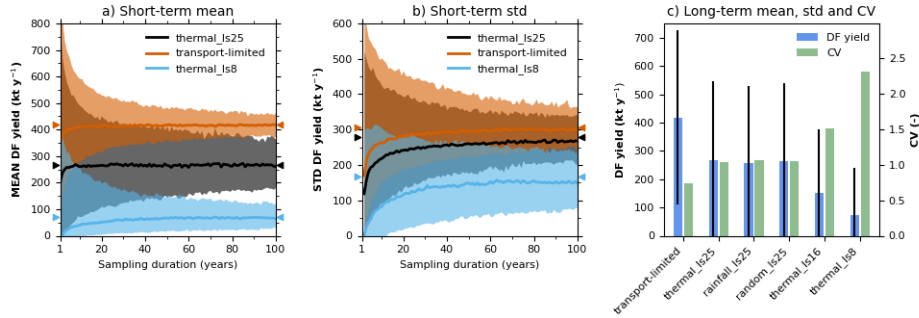


Figure 2. Sensitivity to record duration for (a) mean and (b) standard deviation of annual sediment yields for three scenarios. The medians (solid line) and the 5th-95th percentile range (shaded area) were computed by resampling the 10k-year simulations. Triangles mark the long-term values. (c) The sediment yields long-term mean ± 1 standard deviation (black lines) and coefficient of variation (CV) for all considered scenarios.

202 3.2 Observed and Simulated Debris-Flow Magnitude-Frequency Distri- 203 butions

204 Magnitude-frequency (MF) distributions were estimated for simulated debris-flow
 205 events for all scenarios and compared with observations for the same record duration of
 206 18 years (Figure 3). The distributions are characterized by a power-law tail and range
 207 from $8 \cdot 10^3$ to $7 \cdot 10^5$ m³. The observations lie within the simulated uncertainties of the
 208 transport-limited, thermal_ls25 and thermal_ls8 scenarios. The simulated magnitudes tend
 209 to overestimate observations and this is attributed to the temporal rainfall structure gen-
 210 erated with AWE-GEN and the streamflow that results in these extreme events (Hirschberg,

211 Fatichi, et al., 2021). The power-law tails of the different sediment supply scenarios look
 212 similar, although the actual number of debris-flow events may vary from less than one
 213 to more than four per year (Figure S4). It seems impossible to discern the sediment pro-
 214 duction process from the MF distributions of debris-flow events (Bennett et al., 2014).
 215 However, the magnitudes of the very largest events are significantly different between
 216 the scenarios and point to the fact that the observations are more likely to result from
 217 the supply-limited scenarios (red histograms in Figure 3). The observations, based on
 218 18 years of continuous monitoring, seem to be cutoff at $8 \cdot 10^4 \text{ m}^3$. However, volume es-
 219 timates of destructive debris flows in 1961 suggest the possibility of larger events in the
 220 order of $\sim 5 \cdot 10^5 \text{ m}^3$ (Hürlimann et al., 2003), which are mostly absent in short records.

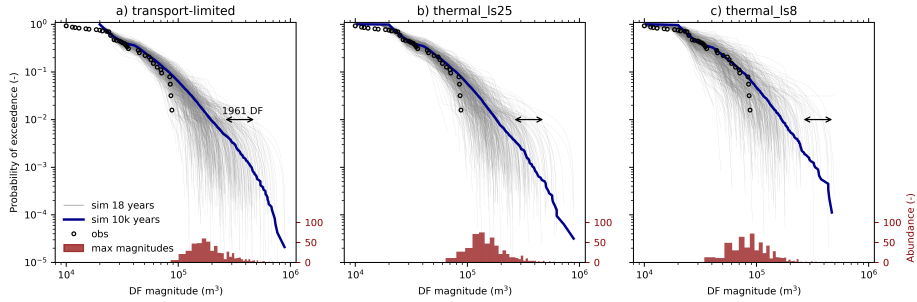


Figure 3. Debris-flow magnitude-frequency distributions. The blue lines were estimated from the 10k-year simulations. The grey lines are fits to 18-year-long subsets of the simulations, which corresponds to the time period of the observations (black circles). The histograms show the largest debris-flow magnitudes (95th percentile) from the simulation subset. The range of volume estimates from large destructive debris flows in 1961 are indicated by the black arrows.

221 3.3 Long-Term Memory Effects in Sediment Fluxes

222 A key premise in this work is that sediment supply limitations may lead to long-
 223 term memory effects in sediment yields. In the DFA, all scenarios show the typical power-
 224 law scaling of the $s-F(s)$ relation (Figure S5). The scaling behavior, expressed as the
 225 exponent α , was more pronounced for short records (Figure 4). This bias for short records
 226 is expected and has no physical meaning (Peng et al., 1994). The presence of long-term
 227 memory is evident in the simulations with stable slopes around $\alpha \approx 0.75$ between ~ 8 -50
 228 years for the ls25 scenarios (Figure 4a,d,e). The scenarios with decreased sediment sup-
 229 ply (thermal_ls26, thermal_ls8) had a shorter period of stable slope (~ 8 -20 years), but
 230 the higher slopes ($\alpha > 0.75$) indicate stronger long-term memory at these timescales
 231 (Figure 4b,c). Depending on the scenario, α scattered more after 20-50 years and trended
 232 towards 0.5, indicating weakening memory and random signals at longer timescales. The
 233 transport-limited scenario differs from all the others because α stabilizes at 0.5 already
 234 for small s . Hence, there are no long-term memory effects in the sediment output induced
 235 by climate, which only imprints a short-term memory signal on sediment yields.

236 Long-term memory is also evident from the uncertainty in $\hat{\mu}$ (Figure 2a). The drop
 237 in uncertainty is inversely related to s for the transport-limited case, while the drop for
 238 the other scenarios is much slower. A similar decrease in the uncertainty for those sce-
 239 narios could only be reproduced by fitting an ARFIMA time series with long-term mem-
 240 ory $H > 0.5$ (Figure S6). Together with the findings of the DFA analysis, this confirms
 241 that the long-term memory in the other scenarios was induced by different sediment sup-
 242 ply regimes.

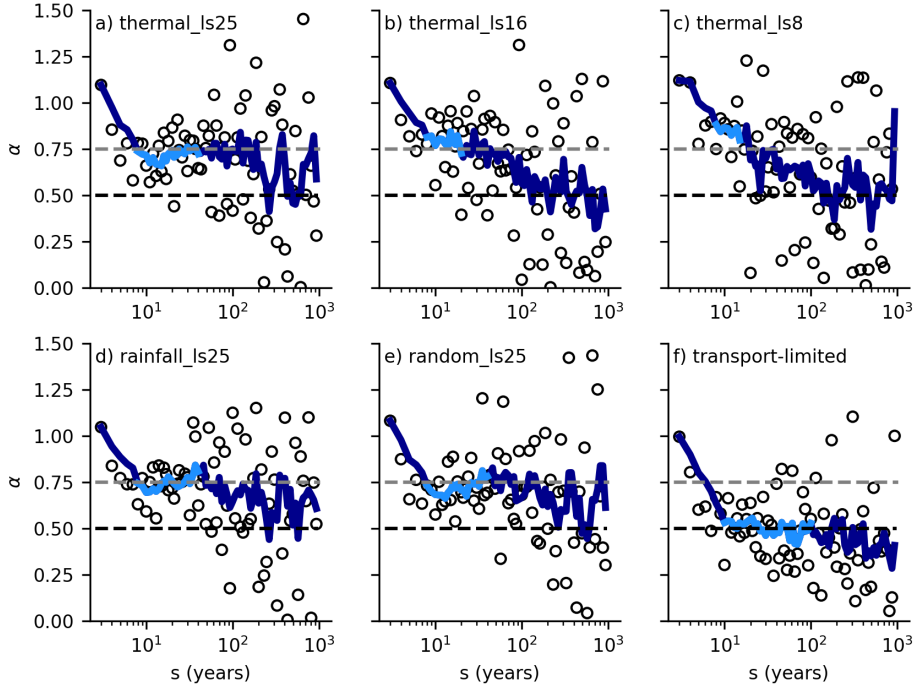


Figure 4. Local slope (exponent α) of the $s - \overline{F(s)}$ relation in sediment yields shown in Figure S5 as a function of sampling duration s . The dots represent the slope between two individual points and the dark blue line is the moving average from five points. The light blue lines mark the timescales with approximately stable slopes (see text). The black dashed line at $\alpha=0.5$ shows the condition of no long-term correlation. The dashed grey line at $\alpha=0.75$ serves for comparison with strong long-term memory being present.

4 Discussion

4.1 Short-Long-Term Discrepancy in Sediment Yield Estimates

We quantified the timescales and amplitude ranges of variabilities in sediment fluxes in Illgraben. We investigated the influence of several different sediment supply scenarios and sampling timescales on sediment yields. Short records (<20 years) resulted in uncertainty in mean ($\hat{\mu}$) and standard deviation ($\hat{\sigma}$) of annual sediment yield of a factor of 2. With current erosion rates, the likelihood of over- or underestimation of $\hat{\mu}$ was balanced. However, in scenarios resulting in more supply-limited conditions, $\hat{\mu}$ was likely to be underestimated if based on short records. The interannual variability $\hat{\sigma}$ was underestimated in all scenarios for short records. This is an inherent effect of undersampling and known from statistics, but compounded by the fact that for supply-limited scenarios, the long-term memory was stronger (Figure 4). If the sediment supply was further decreased, the sediment yield would converge to zero and lose the long-term memory effect. Therefore, interannual variability is expected to be underestimated in short records and geomorphic systems with memory.

Discrepancies between short- and long-term estimates of sediment yield has been attributed to low-frequency high-magnitude pulses of erosion (e.g., Kirchner et al., 2001; Tomkins et al., 2007). Here, we are able to identify what this process is. If it was caused

261 by low-frequency high-magnitude rainfall events leading to large debris flows, the dis-
 262 crepancy would be visible in all scenarios because all scenarios were forced with the same
 263 climate. This points to the role of the stochasticity in hillslope landsliding, which induced
 264 stronger long-term memory for supply-limited scenarios (Figure 4). The discrepancy in
 265 short- and long-term $\hat{\mu}$ in this study was therefore driven by the sequencing of random
 266 large sediment supply events. We acknowledge that our spatially-lumped model neglects
 267 variability in space and is therefore not ideal to study the impact of single extreme rain-
 268 fall events, because the hydrological connectivity may be an important limiting factor
 269 for sediment flux even in small basins (Reid et al., 2007). Nevertheless, the simulated
 270 dynamics reflect observations of elevated debris-flow activity or sediment yield after large
 271 sediment supply events in Illgraben and other basins after landslides (Hürlimann et al.,
 272 2003), earthquakes (e.g., Tang et al., 2011), or wild fires (Cannon et al., 2001), and can
 273 lead to elevated sediment yields even at the 10^3 -year timescale (Korup, 2012).

274 4.2 Implications for Risk Assessment and Mitigation

275 Our findings point to challenges in assessment of climate change impacts on sed-
 276 iment flux, hazard and design of engineering structures (e.g., sediment retention basins),
 277 which are based on short records of sediment yields. Many sediment transport and debris-
 278 flow observation records are short and our simulations have shown the implied risks re-
 279 lated to uncertainties in sediment yields (Figure 2) and underestimating the possibility
 280 of large debris flows (Figure 3). In basins with short records, additional methods and
 281 secondary observations providing information for longer timescales should be consulted.
 282 In debris-flow hazard assessments, events have been reconstructed using dating techniques
 283 such as dendrochronology (e.g., Stoffel et al., 2008) or radiocarbon dating (e.g., Jakob
 284 et al., 2017) to establish MF relationships. Because these methods are time and cost in-
 285 tensive, effort has been put into extrapolating existing MF curves at the regional scale
 286 in relation to morphometric catchment characteristics (de Haas & Densmore, 2019), fan
 287 area, or fan volume (Jakob et al., 2020). In addition to these procedures, stochastic mod-
 288 elling frameworks, as presented here, are helpful for quantifying uncertainties related to
 289 climatic forcing and transient sediment supply and to extend MF distributions beyond
 290 short-term observations (Figure 3).

291 4.3 Preservation of Climate Signals in Sediment Records

292 The sediment supply mechanism (thermal, rainfall or random) in our system had
 293 no effect on the long-term sediment yield estimates. These mechanisms mainly differ in
 294 their timing and seasonality. For example, frost-weathering is most active in cold months
 295 while intense rainfall mainly occurs in warm months. Because the frequency and mag-
 296 nitude of these processes are similar, their differences were not apparent in the sediment
 297 output, and their signals were shredded (Jerolmack & Paola, 2010).

298 Finally, it has been argued that environmental signals will only be recorded and
 299 identified in sediment transport measurements or the sedimentary record if their timescale
 300 exceeds the response time of the system (Castelltort & Van Den Driessche, 2003; Hoff-
 301 mann, 2015), unless the magnitude of the signal exceeds the natural variability (Jerolmack
 302 & Paola, 2010). For Illgraben and similar basins this means that a change needs to per-
 303 sist for only >30 years. This may seem short, but when considering that this catchment's
 304 erosion rate exceeds other Alpine sites by about one order of magnitude (Stutenbecker
 305 et al., 2018; Delunel et al., 2020) and has relatively little opportunity to store sediments
 306 (i.e. only temporary storage), this timescale can be expected to be much larger where
 307 storage opportunities exist and where other controls dominate, such as glacial periods
 308 (e.g., Hoffmann, 2015; Ganti et al., 2016). Stochastic frameworks as presented here are
 309 helpful in quantifying the role of different forcings and future research should aim at quan-
 310 tifying it for other basins with other sediment supply regimes and other geomorphic sys-
 311 tem models.

5 Conclusions

We quantified the uncertainties introduced by climate forcing, transient sediment supply and sampling record duration on estimates of sediment yields in Illgraben by simulating 10k years with a sediment cascade model forced by hourly stochastic weather. Consistent with field observations from other basins, estimates of mean annual sediment yield may be underestimated when based on short records and this effect becomes stronger when the sediment supply is decreased. This results from transient sediment supply by hillslope landslides leading to cycles of transport- and supply-limited conditions. We showed that such cycles cause long-term memory in sediment output at timescales of up to ~50 years. Consequently, the interannual variability of sediment yield estimates was underestimated if sediment supply was limited. Furthermore, we showed that the signal from changing sediment supply mechanisms (triggering conditions), which affect the timing and seasonality of sediment recharge, was shredded. Climate change impacts on sediment supply may therefore only be recorded in the sediment output if they considerably alter the erosion rate of the geomorphic system. The results highlight the importance of characterizing sediment supply events with regard to their stochastic nature. This will support decision making and decrease the risk of misinterpretation both in natural hazard and climate change impact assessments, especially if they are based on short records.

Acknowledgments

This work was partly funded by the WSL research program CCAMM (Climate Change Impacts on Alpine Mass Movements). Data used in this study are available through Hirschberg, Fatichi, et al. (2021) and McArdell and Hirschberg (2020).

References

- Adams, B. A., Whipple, K. X., Forte, A. M., Heimsath, A. M., & Hodges, K. V. (2020). Climate controls on erosion in tectonically active landscapes. *Science Advances*, 6(42). doi: 10.1126/sciadv.aaz3166
- Bak, P., Tang, C., & Wiesenfeld, K. (1987, jul). Self-organized criticality: An explanation of the $1/f$ noise. *Physical Review Letters*, 59(4), 381. Retrieved from <https://journals.aps.org/prl/abstract/10.1103/PhysRevLett.59.381> doi: 10.1103/PhysRevLett.59.381
- Benda, L., & Dunne, T. (1997a). Stochastic forcing of sediment routing and storage in channel networks. *Water Resources Research*, 33(12), 2865–2880. doi: 10.1029/97WR02387
- Benda, L., & Dunne, T. (1997b). Stochastic forcing of sediment supply to channel networks from landsliding and debris flow. *Water Resources Research*, 33(12), 2849–2863. doi: 10.1029/97WR02388
- Bennett, G. L., Molnar, P., Eisenbeiss, H., & Mcardell, B. W. (2012). Erosional power in the Swiss Alps: Characterization of slope failure in the Illgraben. *Earth Surface Processes and Landforms*, 37(15), 1627–1640. doi: 10.1002/esp.3263
- Bennett, G. L., Molnar, P., McArdell, B. W., & Burlando, P. (2014). A probabilistic sediment cascade model of sediment transfer in the Illgraben. *Water Resources Research*, 50(2), 1225–1244. doi: 10.1002/2013WR013806
- Bennett, G. L., Molnar, P., McArdell, B. W., Schlunegger, F., & Burlando, P. (2013). Patterns and controls of sediment production, transfer and yield in the Illgraben. *Geomorphology*, 188, 68–82. Retrieved from <http://dx.doi.org/10.1016/j.geomorph.2012.11.029> doi: 10.1016/j.geomorph.2012.11.029
- Bookhagen, B., & Strecker, M. R. (2012, apr). Spatiotemporal trends in erosion rates across a pronounced rainfall gradient: Examples from the southern Central Andes. *Earth and Planetary Science Letters*, 327–328, 97–110. doi: 10.1016/J.EPSL.2012.02.005

- 363 Borrelli, P., Robinson, D. A., Fleischer, L. R., Lugato, E., Ballabio, C., Alewell, C.,
 364 ... Panagos, P. (2017). An assessment of the global impact of 21st century
 365 land use change on soil erosion. *Nature Communications*, 8(1). Retrieved from
 366 www.nature.com/naturecommunications doi: 10.1038/s41467-017-02142-7
- 367 Bovis, M. J., & Jakob, M. (1999). The role of debris supply conditions in predict-
 368 ing debris flow activity. *Earth Surface Processes and Landforms*, 24(11), 1039–
 369 1054. doi: 10.1002/(SICI)1096-9837(199910)24:11<1039::AID-ESP29>3.0.CO;2
 370 -U
- 371 Brown, E. T., Stallard, R. F., Larsen, M. C., Raisbeck, G. M., & Yiou, F. (1995).
 372 Denudation rates determined from the accumulation of in situ-produced ¹⁰Be
 373 in the luquillo experimental forest, Puerto Rico. *Earth and Planetary Science*
 374 *Letters*, 129(1-4), 193–202. doi: 10.1016/0012-821X(94)00249-X
- 375 Bryce, R. M., & Sprague, K. B. (2012). Revisiting detrended fluctuation analysis.
 376 *Scientific Reports*, 2. doi: 10.1038/srep00315
- 377 Cannon, S. H., Kirkham, R. M., & Parise, M. (2001, aug). Wildfire-related debris-
 378 flow initiation processes, Storm King Mountain, Colorado. *Geomorphology*,
 379 39(3-4), 171–188. doi: 10.1016/S0169-555X(00)00108-2
- 380 Castellort, S., & Van Den Driessche, J. (2003). How plausible are high-frequency
 381 sediment supply-driven cycles in the stratigraphic record? *Sedimentary Geol-*
 382 *ogy*, 157(1-2), 3–13. doi: 10.1016/S0037-0738(03)00066-6
- 383 Coulthard, T. J., & Van De Wiel, M. J. (2013). Climate, tectonics or morphology:
 384 What signals can we see in drainage basin sediment yields? *Earth Surface Dy-*
 385 *namics*, 1(1), 13–27. doi: 10.5194/esurf-1-13-2013
- 386 Covault, J. A., Craddock, W. H., Romans, B. W., Fildani, A., & Gosai, M. (2013).
 387 Spatial and temporal variations in landscape evolution: Historic and longer-
 388 term sediment flux through global catchments. *Journal of Geology*, 121(1),
 389 35–56. doi: 10.1086/668680
- 390 de Haas, T., & Densmore, A. L. (2019). Debris-flow volume quantile predic-
 391 tion from catchment morphometry. *Geology*, 47(8), 1–4. Retrieved from
 392 [https://pubs.geoscienceworld.org/gsa/geology/article/571535/](https://pubs.geoscienceworld.org/gsa/geology/article/571535/Debrisflow-volume-quantile-prediction-from)
 393 [Debrisflow-volume-quantile-prediction-from](https://pubs.geoscienceworld.org/gsa/geology/article/571535/Debrisflow-volume-quantile-prediction-from) doi: 10.1130/G45950.1
- 394 Delunel, R., Schlunegger, F., Valla, P. G., Dixon, J., Glotzbach, C., Hippe, K.,
 395 ... Christl, M. (2020, dec). Late-Pleistocene catchment-wide denudation
 396 patterns across the European Alps. *Earth-Science Reviews*, 211, 103407. Re-
 397 trieved from <https://doi.org/10.1016/j.earscirev.2020.103407> doi:
 398 10.1016/j.earscirev.2020.103407
- 399 Dietrich, W. E., & Dunne, T. (1978). Sediment budget for a small catchment
 400 in mountainous terrain. *Zeitschrift für Geomorphologie*, 29, 191–206. Re-
 401 trieved from <https://www.researchgate.net/publication/247467187> doi:
 402 10.1130/0091-7613(2001)029
- 403 Evans, D. J., Gibson, C. E., & Rossell, R. S. (2006, sep). Sediment loads
 404 and sources in heavily modified Irish catchments: A move towards in-
 405 formed management strategies. *Geomorphology*, 79(1-2), 93–113. doi:
 406 10.1016/j.geomorph.2005.09.018
- 407 Fatichi, S., Ivanov, V. Y., & Caporali, E. (2011). Simulation of future climate
 408 scenarios with a weather generator. *Advances in Water Resources*, 34(4), 448–
 409 467. Retrieved from <http://dx.doi.org/10.1016/j.advwatres.2010.12.013>
 410 doi: 10.1016/j.advwatres.2010.12.013
- 411 Fuller, C. W., Willett, S. D., Hovius, N., & Slingerland, R. (2003). Erosion Rates
 412 for Taiwan Mountain Basins: New Determinations from Suspended Sediment
 413 Records and a Stochastic Model of Their Temporal Variation. *The Journal of*
 414 *Geology*, 111(1), 71–87. doi: 10.1086/344665
- 415 Ganti, V., Hajek, E. A., Leary, K., Straub, K. M., & Paola, C. (2020). Morpho-
 416 dynamic Hierarchy and the Fabric of the Sedimentary Record. *Geophysical Re-*
 417 *search Letters*, 47(14). Retrieved from <https://doi.org/> doi: 10.1029/

418 2020GL087921

- 419 Ganti, V., Von Hagke, C., Scherler, D., Lamb, M. P., Fischer, W. W., & Avouac,
420 J. P. (2016). Time scale bias in erosion rates of glaciated landscapes. *Science*
421 *Advances*, *2*(10). Retrieved from <http://advances.sciencemag.org/> doi:
422 10.1126/sciadv.1600204
- 423 Godard, V., & Tucker, G. E. (2021, sep). Influence of Climate-Forcing Frequency
424 on Hillslope Response. *Geophysical Research Letters*, *48*(18), e2021GL094305.
425 Retrieved from [https://onlinelibrary.wiley.com/doi/full/10.1029/](https://onlinelibrary.wiley.com/doi/full/10.1029/2021GL094305)
426 [2021GL094305](https://onlinelibrary.wiley.com/doi/abs/10.1029/2021GL094305)[https://onlinelibrary.wiley.com/doi/abs/10.1029/](https://onlinelibrary.wiley.com/doi/abs/10.1029/2021GL094305)
427 [2021GL094305](https://agupubs.onlinelibrary.wiley.com/doi/10.1029/2021GL094305) doi: 10.1029/2021GL094305
- 428
- 429 Hirschberg, J., Badoux, A., McArdell, B. W., Leonarduzzi, E., & Molnar, P. (2021).
430 Evaluating methods for debris-flow prediction based on rainfall in an Alpine
431 catchment. *Natural Hazards and Earth System Sciences*, *21*(9), 2773–2789.
432 doi: 10.5194/nhess-21-2773-2021
- 433 Hirschberg, J., Fatichi, S., Bennett, G. L., McArdell, B. W., Peleg, N., Lane, S. N.,
434 ... Molnar, P. (2021). Climate Change Impacts on Sediment Yield and
435 Debris-Flow Activity in an Alpine Catchment. *Journal of Geophysical Re-*
436 *search: Earth Surface*, *126*(1). doi: 10.1029/2020JF005739
- 437 Hoffmann, T. (2015). Sediment residence time and connectivity in non-equilibrium
438 and transient geomorphic systems. *Earth-Science Reviews*, *150*, 609–627. Re-
439 trieved from <http://dx.doi.org/10.1016/j.earscirev.2015.07.008> doi:
440 10.1016/j.earscirev.2015.07.008
- 441 Hovius, N., Stark, C. P., & Allen, P. A. (1997). Sediment flux from a mountain belt
442 derived by landslide mapping. *Geology*, *25*(3), 231–234. doi: 10.1130/0091-
443 -7613(1997)025(0231:SFFAMB)2.3.CO;2
- 444 Hürlimann, M., Rickenmann, D., & Graf, C. (2003). Field and monitoring data
445 of debris-flow events in the Swiss Alps. *Canadian Geotechnical Journal*, *40*(1),
446 161–175. doi: 10.1139/t02-087
- 447 Jakob, M., Bovis, M., & Oden, M. (2005). The significance of channel recharge rates
448 for estimating debris-flow magnitude and frequency. *Earth Surface Processes*
449 *and Landforms*, *30*(6), 755–766. doi: 10.1002/esp.1188
- 450 Jakob, M., Mark, E., McDougall, S., Friele, P., Lau, C. A., & Bale, S. (2020). Re-
451 gional debris-flow and debris-flood frequency–magnitude relationships. *Earth*
452 *Surface Processes and Landforms*. doi: 10.1002/esp.4942
- 453 Jakob, M., Weatherly, H., Bale, S., Perkins, A., & MacDonald, B. (2017). A Multi-
454 Faceted Debris-Flood Hazard Assessment for Cougar Creek, Alberta, Canada.
455 *Hydrology*, *4*(1), 7. doi: 10.3390/hydrology4010007
- 456 Jerolmack, D. J., & Paola, C. (2010). Shredding of environmental signals by sed-
457 iment transport. *Geophysical Research Letters*, *37*(19), 1–5. doi: 10.1029/
458 2010GL044638
- 459 Kantelhardt, J. W., Zschiegner, S. A., Koscielny-Bunde, E., Havlin, S., Bunde, A.,
460 & Stanley, H. E. (2002). Multifractal detrended fluctuation analysis of non-
461 stationary time series. *Physica A: Statistical Mechanics and its Applications*,
462 *316*(1-4), 87–114. doi: 10.1016/S0378-4371(02)01383-3
- 463 Kirchner, J. W., Finkel, R. C., Riebe, C. S., Granger, D. E., Clayton, J. L.,
464 King, J. G., & Megahan, W. F. (2001). Mountain erosion over 10 yr,
465 10 k.y., and 10 m.y. time scales. *Geology*, *29*(7), 591–594. doi: 10.1130/
466 0091-7613(2001)029(0591
- 467 Korup, O. (2012, may). *Earth's portfolio of extreme sediment transport events*
468 (Vol. 112) (No. 3-4). Elsevier. doi: 10.1016/j.earscirev.2012.02.006
- 469 Koscielny-Bunde, E., Bunde, A., Havlin, S., Roman, H. E., Goldreich, Y., &
470 Schellnhuber, H. J. (1998). Indication of a universal persistence law gov-
471 erning atmospheric variability. *Physical Review Letters*, *81*(3), 729–732. doi:
472 10.1103/PhysRevLett.81.729

- 473 Lancaster, S. T., & Casebeer, N. E. (2007). Sediment storage and evacuation in
474 headwater valleys at the transition between debris-flow and fluvial processes.
475 *Geology*, *35*(11), 1027–1030. doi: 10.1130/G239365A.1
- 476 Matsoukas, C., Islam, S., & Rodriguez-Iturbe, I. (2000). Detrended fluctuation anal-
477 ysis of rainfall and streamflow time series. *Journal of Geophysical Research At-*
478 *mospheres*, *105*(D23), 29,165–29,172. doi: 10.1029/2000JD900419
- 479 McArdell, B. W., & Hirschberg, J. (2020). *Debris-flow volumes at the Illgraben 2000-*
480 *2017*. EnviDat. doi: 10.16904/envidat.173
- 481 Molnar, P., & England, P. (1990). Late Cenozoic uplift of mountain ranges and
482 global climate change: Chicken or egg? *Nature*, *346*(6279), 29–34. doi: 10
483 .1038/346029a0
- 484 Montanari, A., Rosso, R., & Taquq, M. S. (1997). Fractionally differenced
485 ARIMA models applied to hydrologic time series: Identification, estima-
486 tion, and simulation. *Water Resources Research*, *33*(5), 1035–1044. doi:
487 10.1029/97WR00043
- 488 Montgomery, D. C., & Runger, G. C. (2018). *Applied statistics and probability for*
489 *engineers*. Wiley Hoboken, NJ.
- 490 Paola, C., Ganti, V., Mohrig, D., Runkel, A. C., & Straub, K. M. (2018). Time
491 Not Our Time: Physical Controls on the Preservation and Measurement of
492 Geologic Time. *Annual Review of Earth and Planetary Sciences*, *46*, 409–438.
493 Retrieved from <https://doi.org/10.1146/annurev-earth-082517-> doi:
494 10.1146/annurev-earth-082517-010129
- 495 Pelletier, J. D., Brad Murray, A., Pierce, J. L., Bierman, P. R., Breshears, D. D.,
496 Crosby, B. T., ... Yager, E. M. (2015). Forecasting the response of Earth’s
497 surface to future climatic and land use changes: A review of methods and
498 research needs. *Earth’s Future*, *3*(7), 220–251. doi: 10.1002/2014EF000290
- 499 Peng, C. K., Buldyrev, S. V., Havlin, S., Simons, M., Stanley, H. E., & Goldberger,
500 A. L. (1994). Mosaic organization of DNA nucleotides. *Physical Review E*,
501 *49*(2), 1685–1689. doi: 10.1103/PhysRevE.49.1685
- 502 Phillips, J. D. (2003). Sources of nonlinearity and complexity in geomorphic
503 systems. *Progress in Physical Geography*, *27*(1), 1–23. doi: 10.1191/
504 0309133303pp340ra
- 505 Reid, S. C., Lane, S. N., Montgomery, D. R., & Brookes, C. J. (2007). Does
506 hydrological connectivity improve modelling of coarse sediment deliv-
507 ery in upland environments? *Geomorphology*, *90*(3-4), 263–282. doi:
508 10.1016/j.geomorph.2006.10.023
- 509 Rydin, & Hassan, G. (2021, jan). *LRydin/MFDFA: v0.4*. Zenodo. Retrieved from
510 <https://doi.org/10.5281/zenodo.4450762> doi: 10.5281/zenodo.4450762
- 511 Sadler, P. M., & Jerolmack, D. J. (2015). Scaling laws for aggradation, denudation
512 and progradation rates: The case for time-scale invariance at sediment sources
513 and sinks. *Geological Society Special Publication*, *404*, 69–88. Retrieved from
514 <http://dx.doi.org/10.1144/SP404.7> doi: 10.1144/SP404.7
- 515 Schaller, M., Von Blanckenburg, F., Hovius, N., & Kubik, P. W. (2001, jun). Large-
516 scale erosion rates from in situ-produced cosmogenic nuclides in European
517 river sediments. *Earth and Planetary Science Letters*, *188*(3-4), 441–458. doi:
518 10.1016/S0012-821X(01)00320-X
- 519 Shao, Z. G., & Ditlevsen, P. D. (2016). Contrasting scaling properties of inter-
520 glacial and glacial climates. *Nature Communications*, *7*, 1–8. doi: 10.1038/
521 ncomms10951
- 522 Stoffel, M., Conus, D., Grichting, M. A., Lièvre, I., & Maître, G. (2008). Unraveling
523 the patterns of late Holocene debris-flow activity on a cone in the Swiss Alps:
524 Chronology, environment and implications for the future. *Global and Planetary*
525 *Change*, *60*(3-4), 222–234. doi: 10.1016/j.gloplacha.2007.03.001
- 526 Stutenbecker, L., Delunel, R., Schlunegger, F., Silva, T. A., Šegvić, B., Girardclos,
527 S., ... Christl, M. (2018). Reduced sediment supply in a fast eroding land-

- 528 scape? A multi-proxy sediment budget of the upper Rhône basin, Central
529 Alps. *Sedimentary Geology*, 375, 105–119. doi: 10.1016/j.sedgeo.2017.12.013
- 530 Tang, C., Zhu, J., Ding, J., Cui, X., Chen, L., & Zhang, J. (2011). Catastrophic
531 debris flows triggered by a 14 August 2010 rainfall at the epicenter of the Wenchuan earthquake. *Landslides*, 8(4), 485–497. doi:
532 10.1007/s10346-011-0269-5
- 533 Tomkins, K. M., Humphreys, G. S., Wilkinson, M. T., Fink, D., Hesse, P. P., Doerr,
534 S. H., . . . Blake, W. H. (2007). Contemporary versus long-term denudation along a passive plate margin: The role of extreme events. *Earth Surface Processes and Landforms*, 32(7), 1013–1031. doi: 10.1002/esp.1460
- 535 Tucker, G. E., & Bras, R. L. (2000). A stochastic approach to modeling the role
536 of rainfall variability in drainage basin evolution. *Water Resources Research*, 36(7), 1953–1964. doi: 10.1029/2000WR900065
- 537 Van De Wiel, M. J., & Coulthard, T. J. (2010). Self-organized criticality in river
538 basins: Challenging sedimentary records of environmental change. *Geology*, 38(1), 87–90. doi: 10.1130/G30490.1
- 539 Wittmann, H., von Blanckenburg, F., Maurice, L., Guyot, J.-L., Filizola, N., &
540 Kubik, P. W. (2011, may). Sediment production and delivery in the Amazon River basin quantified by in situ-produced cosmogenic nuclides
541 and recent river loads. *GSA Bulletin*, 123(5-6), 934–950. Retrieved from
542 <http://www.geosociety.org/pubs/> doi: 10.1130/B30317.1
- 543
544
545
546
547
548